GEOPHYSICS, VOL. 52, NO. 7 (JULY 1987); P. 965–972, 7 FIGS., 1 TABLE.

The critical reflection theorem

Jacob T. Fokkema* and Anton Ziolkowski*

ABSTRACT

In predictive deconvolution of seismic data, it is assumed that the response of the earth is white. Any nonwhite components are presumed to be caused by the source wavelet or by unwanted multiples. We show that this whiteness assumption is invalid at precritical incidence.

We consider plane waves incident on a layered acoustic half-space. At exactly critical incidence at any interface in the half-space, the lower layer acts similar to a rigid plate. The response of the half-space is then all-pass, or white. This result we call the critical reflection theorem. The response is also white if the waves are postcritically incident on the lower half-space. In normal data processing these postcritical components are removed by muting. Thus the whiteness assumption is normally applied to exactly that part of the data where it is invalid.

The demarcation between precritical and postcritical incidence can be exploited for the purposes of deconvolution, provided the data can be decomposed into plane waves. To develop this application, we consider the response of a point source in the uppermost layer of the layered half-space, with a free surface above. The response is simply a superposition of the plane-wave responses already studied, with complications introduced by the source and receiver ghosts and by multiples in the upper layer. At postcritical incidence the earth response is white for all plane-wave components; the source spectrum may be estimated from the postcritical plane-wave components after removing the effects of ghosts and multiples in the upper layer.

If the source signature is already known, the demarcation criterion can be used to separate intrinsic absorption effects from attenuation effects caused by scattering.

INTRODUCTION

In the deconvolution of seismic reflection data it is often assumed that the impulse response of the earth is white and, consequently, that the amplitude spectrum of the data is equal to the amplitude spectrum of the source wavelet. This is exactly what is assumed in routine least-squares prediction-error filtering (Peacock and Treitel, 1969; Robinson and Treitel, 1980, p. 243), especially as it is applied to dynamite data.

We believe there is no theoretical justification for this assumption. The only result we have found that lends any support to the assumption is the all-pass theorem of Treitel and Robinson (1966); but a corollary of the theorem strongly suggests that the whiteness assumption must be wrong, as noted by Ziolkowski and Fokkema (1986).

The all-pass theorem states that the normal-incidence reflection response of a plane-layered earth to an impulsive plane wave is white, provided there is a perfect reflector at the bottom of the stack of layers; that is, provided the reflection coefficient at this reflector is $+1$ or -1. It can easily be seen that this theorem follows from conservation of energy. At the perfect reflector all downgoing energy is reflected back toward the surface. Since none of the elastic layers can create or destroy energy, all the incident energy must eventually return to the surface. This effect is independent of frequency, and therefore the reflection response is all-pass, or white.

There is an important corollary of this all-pass theorem: If there is no perfect reflector in the plane-layered earth, the normal-incidence reflection response to an impulsive plane wave is nonwhite. In practice, even the strongest reflectors in the earth sequence do not have reflection coefficients that are close to $+1$ or -1. Therefore, the normal-incidence impulse response of the real earth is nonwhite.

In this paper we consider nonnormal incidence and an acoustic plane-layered earth model bounded by upper and lower half-spaces. At nonnormal incidence the reflection coefficient can become large, and beyond the critical angle total internal reflection can occur. Since the velocities of the earth

Presented at the 55th Annual International Meeting, Society of Exploration Geophysicists, Washington, D.C. Manuscript received by the Editor March 4, 1985; revised manuscript received December 15, 1986.
*University of Technology Delft, Department of Mining Engineering, P.O. Box 5028, 2600 GA Delft, The Netherlands.

layers generally increase with depth, there will generally be some angle of incidence at which total internal reflection will occur and where all the downgoing incident energy is reflected.

We consider individual plane-wave components of the incident wave and study the structure of the scattered wave. When the downgoing plane wave is critically incident at any interface, the layer below the interface behaves similarly to a rigid plate and reflects all the incident energy. The impulse reflection response of the earth for this plane-wave component is therefore white. We call this result "the critical reflection theorem."

There are a number of corollaries of this theorem, one of which is that the reflection response is nonwhite at precritical incidence; the corollary of the all-pass theorem is a specific case of this result. Another corollary concerns postcritical reflection. If the lower half-space has a velocity greater than that of the upper half-space, there is an incidence angle in the upper half-space for which the wave is critically reflected at the lower half-space. For greater incidence angles, the wave is totally internally reflected at or above the lower half-space and the reflection response is white.

In order to relate these plane-wave results to the seismic reflection method, we consider a monopole source in a layer placed on the layered half-space. The top surface of this uppermost layer is a free surface. The wave field in the uppermost layer may then be expressed as a sum of incident plane-wave components from the source plus a sum of plane-wave components scattered by the layered half-space. The free surface imposes an interference pattern on the scattered field, introducing peaks and notches in the spectrum of the scattered response. The positions of the notches in the spectrum depend upon the depths of the source and receiver and the velocity of the upper layer, while the positions of the peaks depend upon the thickness of the upper layer.

From the structure of the response it is clear that the amplitude spectrum of the source wavelet can be determined from the postcritically reflected plane-wave components of the scattered field. In normal seismic data processing these components are muted out and only precritically reflected components are retained. If the whiteness of the postcritically reflected plane-wave components is to be used for determination of the source spectrum, the data will have to be analyzed in a new way.

THE CRITICAL REFLECTION THEOREM

We consider a stack of N plane-parallel homogeneous acoustic layers, as shown in Figure 1, bounded at the bottom by a homogeneous acoustic half-space of density ρ_{N+1} and velocity v_{N+1}, and at the top by a homogeneous acoustic half-space of density ρ_0 and velocity v_0, where v_0 is less than v_{N+1}. A plane pressure wave is incident from the upper half-space. The normal to the wavefront is parallel to the x-z plane and incident at an angle θ to the normal to the layers, which is chosen to be the z-axis.

The wave propagation is analyzed in the space-frequency domain (x, z, ω) and the complex time factor $\exp(-i\omega t)$ is omitted in the equations.

The incident field is the plane pressure wave

$$p^{\mathrm{INC}}(x, z, \omega) = A_0^-(\omega) \exp\left\{i\omega(p_0 x + q_0 z)\right\}, \tag{1}$$

where $A_0^+(\omega)$ is the spectrum of the pressure wave function, $p_0 = \sin\theta/v_0$ is the horizontal slowness, or ray parameter, in the upper half-space, and $q_0 = (1/v_0^2 - p_0^2)^{1/2}$ is the vertical slowness in the upper half-space. The reflection response of the stratified medium is unknown, but it will be a wave returning at angle θ to the normal, propagating upward:

$$P^R(x, z, \omega) = A_0(\omega) \exp\left\{i\omega(p_0 x - q_0 z)\right\}. \tag{2}$$

The total pressure field in the upper half-space is the sum of the incident and reflected fields:

$$P^0(x, z, \omega) = \exp(i\omega p_0 x) \times \left[A_0^+(\omega) \exp(i\omega q_0 z) + A_0^-(\omega) \exp(-i\omega q_0 z)\right]. \tag{3}$$

The normal component of particle acceleration is related to the pressure gradient by Newton's second law of motion. In the time domain this relationship may be expressed as

$$\frac{d^2 u_z(x, z, t)}{dt^2} = \frac{-1}{\rho} \frac{\partial p(x, z, t)}{\partial z}, \tag{4}$$

where $u_z(x, z, t)$ is the normal component of particle displace-

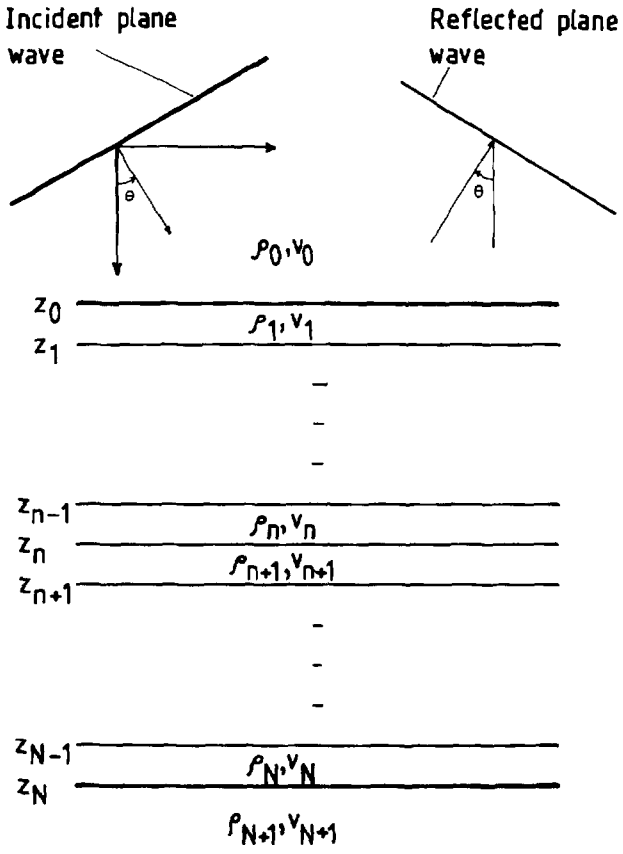

Fig. 1. A stack of plane-parallel homogeneous acoustic layers bounded at the bottom by a homogeneous acoustic half-space of density ρ_{N+1} and velocity v_{N+1}, and at the top by a homogeneous acoustic half-space of density ρ_0 and velocity v_0. v_0 is less than v_{N+1}. A plane pressure wave is incident from the upper half-space; the normal to the wavefront is parallel to the x-z plane at an angle θ to the normal to the layers, which is the z-axis.

ment. For a plane wave, the total differentiation with respect to time d/dt is equal to the partial derivative $\partial/\partial t$, and equation (4) may be transformed to the frequency domain to yield

$$U_z(x, z, \omega) = \frac{1}{\rho\omega^2}\frac{\partial P(x, z, \omega)}{\partial z}. \tag{5}$$

Thus, in the upper half-space, layer 0, the normal component of displacement, is

$$U_z^0(x, z, \omega) = \frac{iq_0}{\rho_0\omega}\exp(i\omega p_0 x) \times\left[A_0^+(\omega)\exp(i\omega q_0 z) - A_0^-(\omega)\exp(-i\omega q_0 z)\right]. \tag{6}$$

Similarly, the pressure and normal displacement fields in the nth and $(n+1)$th layers are

$$P^n(x, z, \omega) = \exp(i\omega p_n x) \times\left[A_n^+(\omega)\exp(i\omega q_n z) + A_n^-(\omega)\exp(-i\omega q_n z)\right] \tag{7}$$

and

$$U_z^n(x, z, \omega) = \frac{iq_n}{\rho_n\omega}\exp(i\omega p_n x) \times\left[A_n^+(\omega)\exp(i\omega q_n z) - A_n^-(\omega)\exp(-i\omega q_n z)\right] \tag{8}$$

for all values of x and for $z_{n-1} \le z \le z_n$, and

$$P^{n+1}(x, z, \omega) = \exp(i\omega p_{n+1} x) \times\left[A_{n+1}^+(\omega)\exp(i\omega q_{n+1} z) + A_{n+1}^-(\omega)\exp(-i\omega q_{n+1} z)\right] \tag{9}$$

and

$$U_z^{n+1}(x, z, \omega) = \frac{iq_{n+1}}{\rho_{n+1}\omega}\exp(i\omega p_{n+1} x) \times\left[A_{n+1}^+(\omega)\exp(i\omega q_{n+1} z) - A_{n+1}^-(\omega)\exp(-i\omega q_{n+1} z)\right] \tag{10}$$

for all values of x and $z_n \le z \le z_{n+1}$.

From the continuity of pressure at the boundaries for all values of x, it follows that

$$p_0 = p_1 = \cdots = p_n = p_{n+1} = \cdots p_{N+1}, \tag{11}$$

which is Snell's law. It can be expressed as

$$p_n = \frac{\sin\theta}{v_0} = p, \qquad \text{for} \quad n = 1, 2, 3, \ldots, N+1. \tag{12}$$

Since

$$q_n = \left(\frac{1}{v_n^2} - p^2\right)^{1/2},$$

q_n will become imaginary if $p > 1/v_n$. At each boundary, pressure and displacement are continuous. That is,

$$\lim_{z \uparrow z_n} P^n(x, z, \omega) = \lim_{z \downarrow z_n} P^{n+1}(x, z, \omega), \tag{13}$$

and

$$\lim_{z \uparrow z_n} U_z^n(x, z, \omega) = \lim_{z \downarrow z_n} U_z^{n+1}(x, z, \omega). \tag{14}$$

We now define a global reflection coefficient $R_n(\omega)$ for the nth layer as follows:

$$A_n^-(\omega) = R_n(\omega)A_n^+(\omega)\exp(2i\omega q_n z_n). \tag{15}$$

Divide equation (14) by equation (13), after substitution from expressions (7), (8), (9), and (10), using equation (15) and a similar expression for the $(n+1)$st layer to obtain the following recursion formula for the global reflection coefficient.

$$R_n(\omega) = \frac{\Gamma_n + R_{n+1}(\omega)\exp\left\{i\omega\tau_{n+1}\right\}}{1 + \Gamma_n R_{n+1}(\omega)\exp\left\{i\omega\tau_{n+1}\right\}}, \tag{16}$$

in which

$$\tau_{n+1} = 2q_{n+1}(z_{n+1} - z_n) \tag{17}$$

is the vertical two-way traveltime in layer n, and

$$\Gamma_n = \frac{q_n/\rho_n - q_{n+1}/\rho_{n+1}}{q_n/\rho_n + q_{n+1}/\rho_{n+1}} \tag{18}$$

is the local reflection coefficient. [It can be seen that when $p = 0$, $q_n = 1/v_n$, $q_{n+1} = 1/v_{n+1}$, and equation (18) is the well-known expression for the reflection coefficient at normal incidence.] Using definition (15) for the upper half-space, equation (3) may be written as

$$P_0(x, z, \omega) = A_0^+(\omega)\exp(i\omega p x) \times\left[\exp(i\omega q_0 z) + R_0(\omega)\exp\left\{i\omega q_0(2z_0 - z)\right\}\right]. \tag{19}$$

At critical incidence at the interface $z = z_n$, $p_{n+1} = p = 1/v_{n+1}$ by definition, from which it follows that $q_{n+1} = 0$. Equation (10) shows that the particle displacement $U_z^{n+1}(x, z, \omega) = 0$ for all frequencies, for all values of x, and for $z_n \le z \le z_{n+1}$. That is, the $(n+1)$th layer acts similarly to a rigid plate at critical incidence, and it follows that all the incident energy will be returned to the surface.

This conclusion can be drawn from the recursion formula (16) and the auxiliary equation (18). When $q_{n+1} = 0$, $\Gamma_n = 1$, and therefore $R_n(\omega) = 1$ for all ω. The recursion formula (16) then gives

$$R_{n-1}(\omega) = \frac{\Gamma_{n-1} + \exp\left\{i\omega\tau_n\right\}}{1 + \Gamma_{n-1}\exp\left\{i\omega\tau_n\right\}}, \tag{20}$$

in which Γ_{n-1} is real with modulus less than 1. The numerator and denominator of the right-hand side of equation (20) are complex numbers which have the same modulus, but different phases. Therefore, $R_{n-1}(\omega)$ is a complex number of modulus 1. It follows that $R_{n-2}(\omega)$, $R_{n-3}(\omega)$, ..., $R_0(\omega)$ are all modulus 1. From equation (15), it follows that the amplitude spectrum of the total field in the upper half-space is the same as the spectrum of the incident pressure wave, and the reflection response of the layered sequence is therefore white.

COROLLARIES

Corollary 1: At precritical incidence, the response is nonwhite.

At precritical incidence, Γ_n is real and has modulus less than 1 for all layers. Therefore, there is a wave transmitted into the lower half-space. There cannot be any upcoming waves in the lower half-space; therefore, $R_{N+1}(\omega) = 0$, and it follows from the recursion equation (16) that $R_N(\omega) = \Gamma_N$ which has modulus less than 1 and is real. Using the recursion again, it follows that $R_{N-1}(\omega)$ is complex and frequency-dependent, with modulus less than 1. Following the recursion to the top of the stack with all Γ_n real and modulus less than 1, it follows that all the $R_n(\omega)$ are complex with modulus less than 1, including $R_0(\omega)$. Therefore the reflection response is not white.

Corollary 2: At precritical incidence, the reflection response is, in general, not minimum-phase.

Applying the recursion formula (16) to the upper half-space yields

$$R_0(\omega) = \frac{\Gamma_0 + R_1(\omega)\exp(i\omega\tau_1)}{1 + \Gamma_0 R_1(\omega)\exp(i\omega\tau_1)}, \tag{21}$$

in which, from corollary 1, we established that $|\Gamma_0| < 1$ and $|R_1(\omega)| < 1$. The denominator of equation (21) is minimum-phase and therefore $R_0(\omega)$ is causal. This is a generalization of the normal-incidence result found by Treitel and Robinson (1966). For $R_0(\omega)$ to be minimum-phase, we require also that $|R_1(\omega)| < |\Gamma_0|$, which will not generally be the case. It follows that $R_0(\omega)$ is not in general minimum-phase.

Corollary 3: If there are only evanescent waves in the lower half-space, the reflection response is white.

Since $v_0 < v_{N+1}$, it is possible to have an incident wave in the upper half-space such that

$$p = \frac{\sin\theta_0}{v_0} > \frac{1}{v_{N+1}}. \tag{23}$$

It follows that $q_{N+1} = i(p^2 - 1/v_{N+1}^2)^{1/2}$ is pure imaginary, and therefore, from equation (18), Γ_N is complex and has modulus 1. In the lower half-space there are no upcoming waves, so $R_{N+1}(\omega) = 0$ and therefore, in equation (16), $R_N(\omega) = \Gamma_N$, which is complex and has modulus 1. Following the recursion (16) upward, it follows that $R_{N-1}(\omega)$, $R_{N-2}(\omega)$, ..., $R_0(\omega)$ are all complex and have modulus 1. Therefore the reflection response is white.

SYNTHETIC EXAMPLES

We now demonstrate the effect of varying the angle of incidence on the plane-wave reflection response in two examples. In the first example we use a real well log from the North Sea

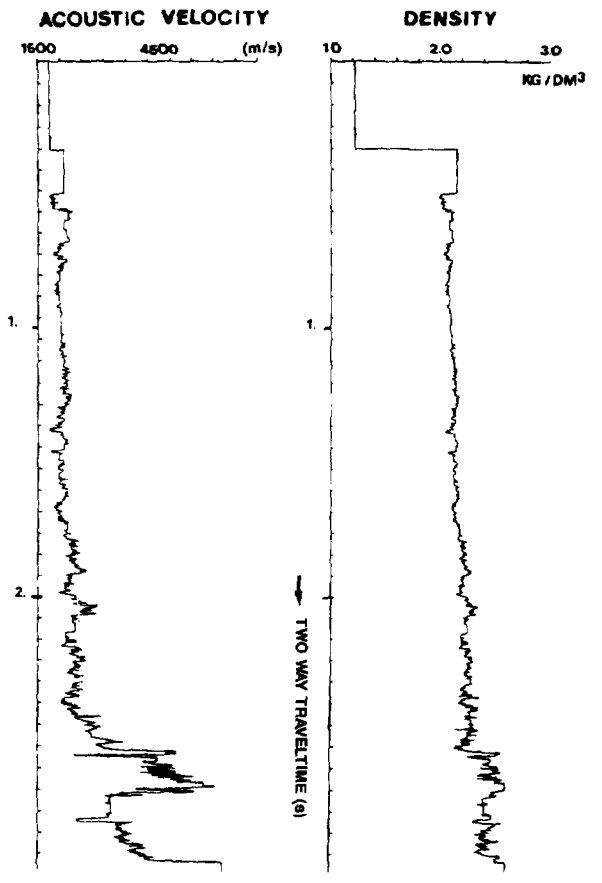

FIG. 2. Velocity and density logs from a North Sea well, subdivided into 684 discrete layers of different thicknesses.

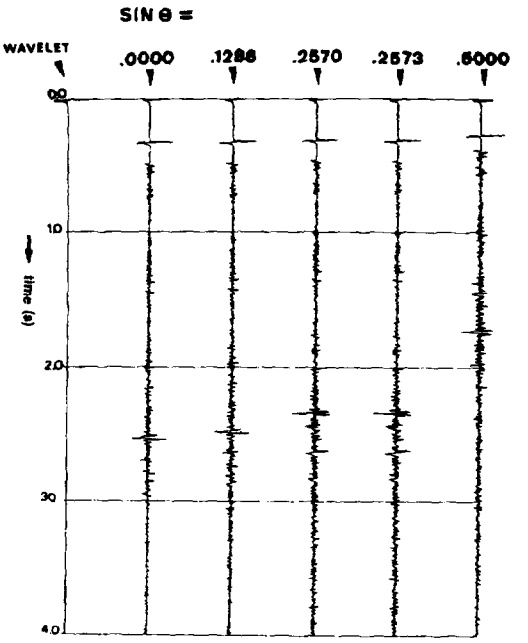

FIG. 3. The incident-wave and plane-wave reflection responses from the horizontally layered structure described by the profiles of Figure 2: (a) the incident wavelet; (b) the normally incident reflection response; (c) a precritical reflection response; (d) a precritical reflection response just before critical reflection; (e) a postcritical reflection response just after critical reflection; (f) a postcritical reflection response at a large angle of incidence (30 degrees).

which has been represented as 684 horizontal acoustic layers. In the second example we take a simple five-layer case.

(1) 684-layer case

The acoustic velocity and density profiles are shown in Figure 2. The incident wavelet and the plane-wave reflection responses at various angles of incidence are shown in Figure 3. The lower half-space has the highest velocity, and the wave is critically reflected at the lower half-space when the angle of incidence is arcsin (0.25713) in the upper half-space. The reflection responses in Figure 3 are thus divided into three precritical and two postcritical responses, with the responses at $\sin\theta = 0.2570$ and $\sin\theta = 0.2573$ corresponding to just before and just after critical reflection in the lower half-space. Notice how similar these two responses are. The response at $\sin\theta = 0.5$ becomes critically reflected at a layer shallower than the lower half-space.

In Figure 4 we show the amplitude spectra of the incident wavelet and the reflection responses. The two postcritical responses have the same amplitude spectrum as the incident wavelet, showing that the reflection response of the sequence is white (corollary 3). The three precritical responses have different spectra; therefore, the precritical earth response is not white (corollary 1). Notice that, although the two responses just before and just after critical reflection are very similar in the time domain, their spectra are dramatically different.

(2) Five-layer case

We now consider a much simpler case, with only five layers (Table 1). The incident wavelet and five reflection responses are shown in Figure 5. The incident wave is critically reflected at the lower half-space when the angle of incidence in the upper half-space is 30 degrees (arcsin 0.5). Three precritically and two postcritically reflected responses are shown, with the last precritical response ($\sin\theta = 0.499$) and the first postcritical response ($\sin\theta = 0.501$) looking very similar. The corresponding amplitude spectra of these responses are shown in Figure 6. Once again, we see that the spectra of the postcritical responses are the same as the spectrum of the incident wavelet, while the spectra of the precritical reflection responses are different. It follows that the postcritical reflection response of the earth is white, while the precritical reflection response is nonwhite.

Table 1. Velocity and density structure of the five-layer model used in the second synthetic example.

Layer	Depth	Velocity (m/s)	Density (kg/m^3)
Upper half-space	≤ 0	1500	1000
1	0–300	1800	1000
2	300–600	2100	1000
3	600–900	2400	1000
4	900–1200	2000	1000
5	1200–1500	2500	1000
Lower half-space	≥ 1500	3000	1000

POINT-SOURCE RESPONSE AND THE INFLUENCE OF THE FREE SURFACE

In order to relate the plane-wave results to the seismic reflection method, we now use the earth model shown in Figure 7, in which the upper half-space of Figure 1 has been replaced by a layer with a free surface at $z = 0$. This upper layer has the same velocity and density as the upper half-space of Figure 1. We introduce a monopole source in this layer at a depth h_s on the z-axis.

The pressure in this uppermost layer consists of an incident field P^{INC} and a scattered field P^s:

$$P_0(p_x, p_y, z, \omega) = P^{INC}(p_x, p_y, z, \omega) + P^s(p_x, p_y, z, \omega), \quad (21)$$

in which we introduce the third dimension y. The incident field satisfies the inhomogeneous wave equation

$$\frac{\partial^2 P^{INC}}{\partial z^2} + \omega^2 q_0^2 P^{INC} = -S(\omega)\delta(z - h_s), \quad (22)$$

in which $q_0 = ((1/v_0^2) - p_x^2 - p_y^2)^{1/2}$ from cylindrical symmetry,

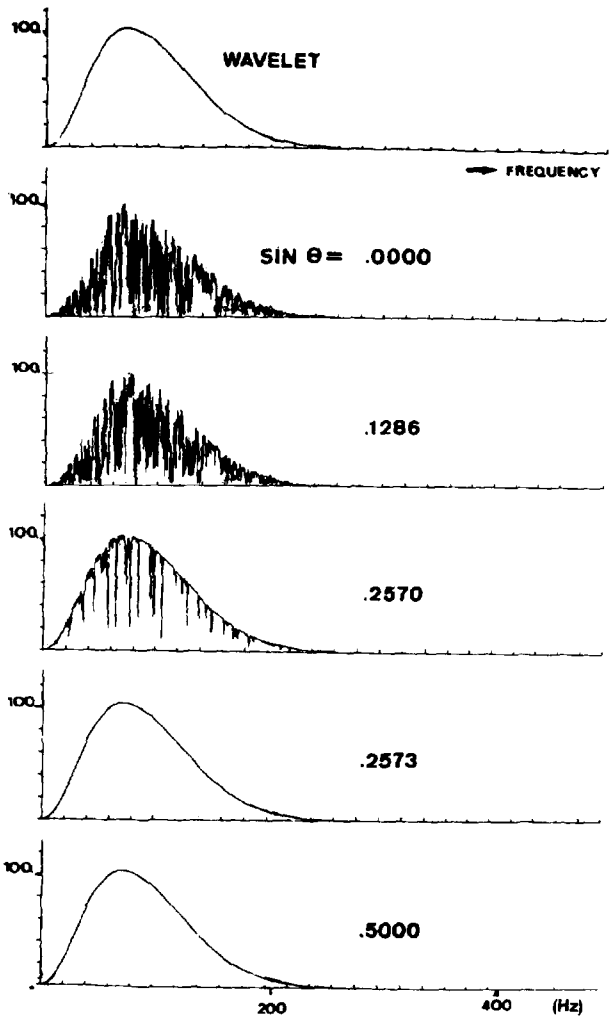

FIG. 4. The amplitude spectra (a)–(f) of the traces (a)–(f), respectively, in Figure 3.

and $S(\omega)$ is the source spectrum. The well-known solution of equation (22) is

$$P^{INC} = i\frac{S(\omega)}{2\omega q_0}\exp\left[i\omega(p_x x + p_y y + q_0|z - h_s|)\right], \quad (23)$$

for $0 \le z \le z_0$.

The factor $\exp[i\omega(p_x x + p_y y)]$ *is common to both the incident and scattered fields and will be omitted in further equations, for simplicity.* The scattered field consists of upgoing and downgoing waves, as in the other layers:

$$P^s = A_0^+ \exp\left[i\omega q_0 z\right] + A_0^- \exp\left[i\omega(2q_0 z_0 - q_0 z)\right] \quad (24)$$

for $0 \le z \le z_0$.

We now find the global reflection coefficient R_0 at the boundary $z = z_0$. As before, this is the ratio of the upgoing wave to the downgoing wave, but now recognizing that the downgoing wave consists of both the incident wave and a scattered wave,

$$A_0^- = R_0\left[i\frac{S(\omega)}{2\omega q_0}\exp(-i\omega q_0 h_s) + A_0^+\right]. \quad (25)$$

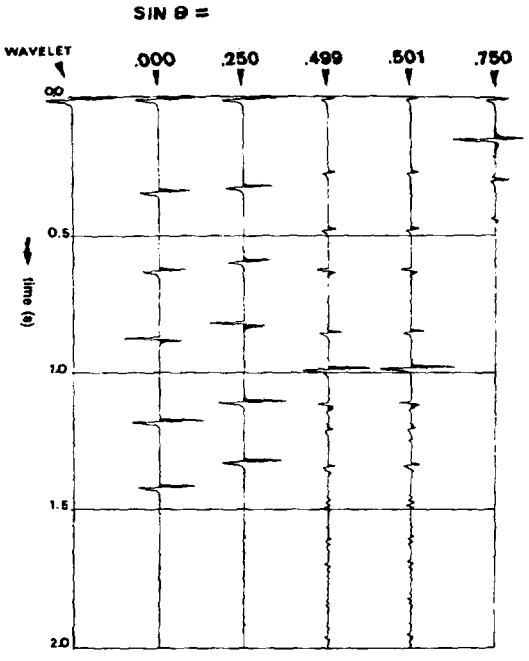

FIG. 5. The incident-wave and plane-wave reflection responses from a five-layer model (Table 1): (a) the incident wavelet; (b) the normal incidence reflection response; (c) a precritical reflection response; (d) a precritical reflection response just before critical reflection; (e) a postcritical reflection response just after critical reflection; (f) a postcritical reflection response at a large angle of incidence.

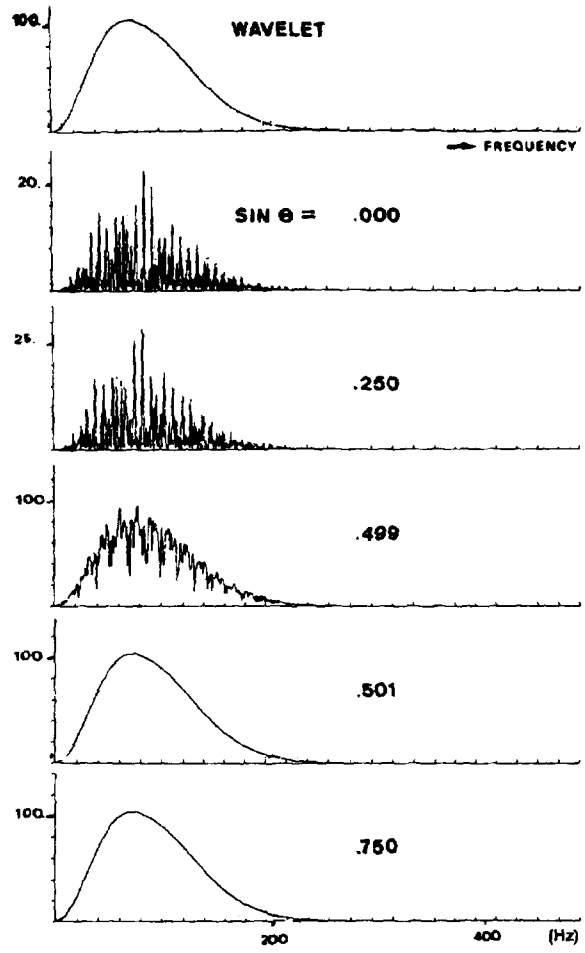

FIG. 6. The amplitude spectra (a)–(f) of traces (a)–(f), respectively, in Figure 5.

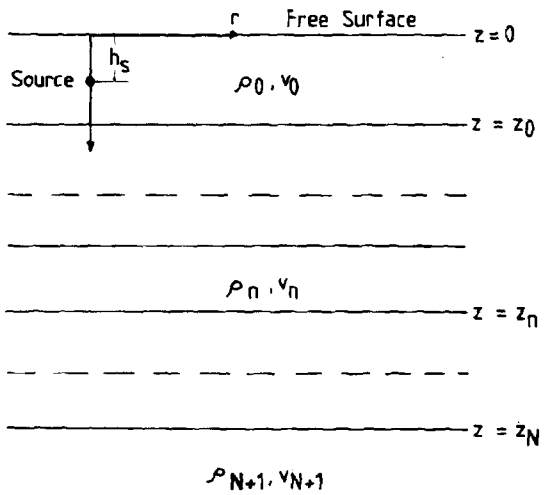

FIG. 7. A point source is introduced into the uppermost layer, layer 0, which has a free surface at $z = 0$. The layered halfspace is otherwise identical with that shown in Figure 1.

At the free surface $z = 0$, the boundary condition is that the pressure is zero:

$$P_0 = 0. \tag{26}$$

Therefore, from equations (21), (23), and (24) it follows that

$$A_0^- \exp(2i\omega q_0 z_0) = -1\left[i \frac{S(\omega)}{2q_0 \omega} \exp(i\omega q_0 h_s) + A_0^+ \right] \tag{27}$$

in which the well-known (-1) reflection coefficient is clearly recognizable. Equations (25) and (27) can be solved for A_0^- and A_0^+, thus enabling the scattered field P^s in equation (24) to be determined. Combining this result with equation (23) yields the complete expression for the total field in layer 0 at a depth z, as follows:

$$P_0(p, z, \omega) = S(\omega)G(p, z, \omega) \tag{28}$$

in which $P = (P_x^2 + P_y^2)^{1/2}$ and the Green's function $G(p, z, \omega)$ are given by

$$G(p, z, \omega) = \frac{i}{2\omega q_0}\left[G^{\text{INC}}(p, z, \omega) + G^s(p, z, \omega) \right], \tag{29}$$

where

$$G^{\text{INC}}(p, z, \omega) = \exp\left[i\omega q_0 |z - h_s| \right] - \exp\left[i\omega q_0 (z + h_s) \right] \tag{30}$$

and

$$G^s(p, z, \omega) = \frac{R_0 \exp\left[i\omega q_0 (2z_0 - z - h_s) \right]}{1 + R_0 \exp(2i\omega q_0 z_0)} \times \left[1 - \exp(2i\omega q_0 h_s) \right]\left[1 - \exp(2i\omega q_0 z) \right]. \tag{31}$$

The Green's function consists of an incident field and a scattered field. The incident field contains two terms, described by equation (30): The first term is the direct wave from the source; and the second term is the reflection of this wave in the free surface (the ghost). The scattered field is described by equation (31) and contains five factors: R_0 is, of course, the global reflection coefficient at $z = z_0$ and contains all the information about the layered half-space; the denominator describes the behavior of the multiples in the first layer; the factor $[1 - \exp(2i\omega q_0 h_s)]$ is the ghost operator at the source; the factor $[1 - \exp(2i\omega q_0 z)]$ is the ghost operator at the receiver; and $\exp[i\omega q_0 (2z_0 - z - h_s)]$ is simply a phase factor.

We may also find an expression for the vertical component of the particle velocity $\dot{U}_z$ in the layer, using the relation

$$\dot{U}_z(p, z, \omega) = \frac{1}{i\omega\rho_0} \frac{\partial P_0(p, z, \omega)}{\partial z}. \tag{32}$$

The interesting case for exploration geophysics is for $z = 0$, corresponding to the situation where geophones are placed on the surface. Here,

$$\frac{i\omega\rho_0 \dot{U}_z(p, 0, \omega)}{S(\omega)} = \exp(i\omega q_0 h_s) + \frac{R_0 \exp\left[i\omega q_0 (2z_0 - h_s) \right]}{1 + R_0 \exp(2i\omega q_0 z_0)} \times \left[1 - \exp(2i\omega q_0 h_s) \right]. \tag{33}$$

The direct wave and its free-surface reflection combine to give a single term $[\exp(i\omega q_0 h_s)]$ for the incident field. In the scattered field the multiples and source ghost operator are still there, but the receiver ghost vanishes since the geophones are at the surface.

DISCUSSION AND CONCLUSIONS

The critical reflection theorem yields a demarcation between plane-wave components that are precritically and postcritically incident on the lower half-space of an acoustic plane-layered earth model. At precritical incidence, the reflection response is nonwhite; however, at postcritical incidence, there are only evanescent waves in the lower half-space, and the reflection response is white.

This result has an obvious application to the deconvolution of seismic data, when the wavelet is minimum-phase. It is usually assumed that the spectrum of the wavelet may be obtained from the data, if the earth reflection response is white, random, and stationary (for example, Robinson and Treitel, 1980, p. 243). We have now proven that the reflection response at precritical incidence is not white. Therefore, the whiteness assumption does not hold at precritical incidence. The assumptions of randomness and stationarity are irrelevant: If the earth reflection response is random and stationary, but not white, the spectrum of the reflected data is not the same as the spectrum of the incident wavelet; if the earth reflection response is white, but not necessarily random or stationary, the spectrum of the reflected data is the same as the spectrum of the incident wavelet. We can see from our two examples that the number of layers, stationarity, and randomness are irrelevant; it matters only whether the plane waves are precritically or postcritically reflected at the lower half-space.

If the data can be treated as a point source over a layered half-space, the source can be decomposed into its plane-wave components (as described in the previous section). In shot gathers over structures with significant dip, the plane, horizontally layered earth model may be a poor approximation to the real earth. We suggest that this model is a better fit to common-midpoint (CMP) gathers, in which the effect of dip is minimized (see, for example, Diebold and Stoffa, 1981). The CMP gather then looks like a shot gather over an *equivalent* plane-layered earth model, as described by Figure 7.

The measured pressure field $\tilde{P}(r, z, t)$, in which r is the shot-receiver offset in the CMP gather, may then be transformed to frequency to yield $\tilde{P}(r, z, \omega)$. The cylindrical symmetry about the z-axis through the source allows the data to be transformed from offset r to wavenumber k_r, via the

Hankel transform (see Bracewell, 1965, p. 248):

$$\tilde{\tilde{P}}_0(k_r, z, \omega) = \int_0^\infty \tilde{P}_0(r, z, \omega) J_0(rk_r) r \, dr, \tag{34}$$

where k_r is chosen for appropriate p values, in which

$$k_r = \omega p. \tag{35}$$

Thus we find

$$P_0(p, z, \omega) = \int_0^\infty \tilde{P}(r, z, \omega) J_0(\omega p r) r \, dr, \tag{36}$$

in which $P_0(p, z, \omega)$ has the structure described by equation (28).

After the incident field has been removed (this could even be done before the Hankel transformation), the individual plane-wave responses of the scattered field can be analyzed. Using the demarcation provided by the critical reflection theorem, $|R_0| = 1$ for any ray parameter p greater than $p_{crit} = 1/v_{N+1}$, where v_{N+1} is the velocity in the lower half-space. In the time domain, each of these plane-wave components consists of a source wavelet convolved with the white reflection response, and further convolved with a source ghost operator, a receiver ghost operator, and an operator describing the multiples in the first layer. A band-limited amplitude spectrum of the source wavelet may now be extracted from these plane-wave components using the methods of predictive deconvolution. If the wavelet is minimum-phase (in the case of dynamite, for example), it may be calculated from the amplitude spectrum using standard methods. Finally, the precritical plane-wave components can now be deconvolved using this wavelet derived from the postcritical plane-wave components.

In normal seismic data processing the muting process before stack removes all postcritical plane-wave components. In other words, in standard predictive deconvolution the whiteness assumption is applied on precisely the part of the data where it is invalid. Our proposal simply involves splitting the data into two parts: precritical incidence and postcritical incidence. The precritical data are more or less what is left after muting, and the postcritical data are what is normally removed. It is only at postcritical incidence that the whiteness assumption is valid.

In all of the above we have been dealing with lossless media, but absorption may also take place. Absorption can only be studied when the frequency-dependent elastic effects are taken into account first (Ziolkowski and Fokkema, 1986). We can check for the effects of absorption if we know the spectrum of the incident plane wave. If the spectra of the plane-wave decomposed data at postcritical incidence are compared with the spectrum of the incident wavelet, attenuation of the incident spectrum should be observed in the reflected data if absorption is present. Any effects of absorption can be identified with specific layers by considering different postcritical angles. As the velocities generally increase with depth, the largest p values correspond to total internal reflections in the shallowest layers, while decreasing p values contain data from deeper layers.

In conclusion, the postcritically reflected data, which are muted out in conventional processing, contain valuable information which can also be used in the processing of the precritically reflected data. We emphasize that the assumption of whiteness cannot be applied to the precritical earth reflection response.

ACKNOWLEDGMENTS

We thank Frits Leyds for performing the calculations shown in our synthetic examples, and for preparing the diagrams. We also thank the Triple Society for moral support. The work was supported financially by the European Economic Community under contract number TH 01.39/84.

REFERENCES

Bracewell, R., 1965, The Fourier transform and its applications: McGraw-Hill Book Co., Inc.

Diebold, J. B., and Stoffa, P. L., 1981, The traveltime equation, tau-p mapping, and inversion of common-midpoint data: Geophysics, **46**, 238–254.

Peacock, K. L., and Treitel, S., 1969, Predictive deconvolution: Theory and practice: Geophysics, **34**, 155–169.

Robinson, E. A., and Treitel, S., 1980, Geophysical signal analysis: Prentice-Hall, Inc.

Treitel, S., and Robinson, E. A., 1966, Seismic wave propagation in terms of communication theory: Geophysics, **31**, 17–32.

Ziolkowski, A., and Fokkema, J. T., 1986, The progressive attenuation of high-frequency energy in seismic reflection data: Geophys. Prosp., **34**, 981–1001.